Hindawi
Complexity
Volume 2022, Article ID 6795101, 10 pages
https://doi.org/10.1155/2022/6795101

WILEY | Hindawi

Research Article

A Novel Mining Approach for Data Analysis and Processing Using Unmanned Aerial Vehicles

Ali Alenezi,[1,2] **Ahmad Sawalmeh**,[2,3] **Hazim Shakhatreh**,[4] **Muhannad Almutiry**,[1,2] **and Nasser Aedh Alreshidi**[5]

[1]*Department of Electrical Engineering, Northern Border University, Arar, Saudi Arabia*
[2]*Remote Sensing Unit, Northern Border University, Arar, Saudi Arabia*
[3]*Computer Science Department, Northern Border University, Arar, Saudi Arabia*
[4]*Department of Telecommunications Engineering, Hijjawi Faculty for Engineering Technology, Yarmouk University, Irbid, Jordan*
[5]*Department of Mathematics, College of Science, Northern Border University, Arar, Saudi Arabia*

Correspondence should be addressed to Hazim Shakhatreh; hazim.s@yu.edu.jo

Received 2 March 2022; Revised 3 May 2022; Accepted 5 May 2022; Published 18 May 2022

Academic Editor: Chao Zeng

In the mining industry, smart surveying and exploration operations for the minerals are essential during mining missions. Usually, these missions are performed in remote areas that do not have a wireless communications infrastructure. This paper proposes to use the unmanned aerial vehicle (UAV) as a relay communication node between the exploration team and the ground control station (GCs). UAV can act as a relay node to provide mobile, flexible, and reliable communication links in remote environments and complex topologies. In this work, the pathloss models in millimeter-wave technology are considered because they provide massive data rates for line of sight scenarios. The optimization problem of identifying a 3D location and trajectory of the UAV relay node is formulated to maximize the total team members' data rate. Because the problem is non-convex, the particle swarm optimization algorithm is used to solve it and determine an efficient location and trajectory of the UAV.

1. Introduction

Unmanned Aerial Vehicles (UAVs) have recently been employed in a variety of civilian applications, including real-time monitoring, infrastructure inspection, remote sensing, search and rescue operations, cargo delivery, surveillance, precision agriculture, and assisting with wireless coverage [1]. The UAV can be used for a variety of purposes in wireless communications, including providing coverage in the scenario of a base station failure during a disaster or temporary congestion in a specific geographic area [2–4].

On the one hand, numerous studies use UAVs as wireless communication relay nodes. For example, the analysis in [5] proposed employing a UAV as a relay to lower UAV transmission power. In addition, the team designed an energy-efficient relay UAV deployment in [6], which reduces backhaul link capacity and backhaul link latency. Kumar et al. [7] also addressed utilizing a UAV as a relay communication node to guarantee the quality of service requirements was met. Furthermore, the authors devised a closed-form to discover the optimal position of the UAV acting as a relay in [8], to maximize network reliability. In [9], the authors study the problem of locating an aerial relay node efficiently that is presented as an optimization problem, with the goal of maximizing total wireless device throughput. When conventional base stations' capacity is suffering in some extreme scenarios, such as congestion inside the cell or a particular event, the authors of [10] propose an efficient three-dimensional placement of a single UAV-assisted wireless network. The goal of the research is to determine the 3D location of the UAV base station as well as the percentage of available bandwidth that must be allocated to the UAV in order to maximize the number of users serviced. The authors of [11] investigate a UAV-enabled uplink NOMA network in which the UAV receives data from ground users while flying at a predetermined altitude.

They study the topic of user pairing and provide a dynamic power allocation technique for calculating the user's power allocation coefficients, as well as a closed-form equation for the ergodic sum rate. In [12], the authors utilize a cell on wheels that cooperates with a single UAV in order to provide maximum wireless coverage to ground users.

On the other side, Zhan et al. proposed in [8] a multi-UAV relaying network between a group of users and a distant base station to establish a single-hop communication between ground users and the base station. In this work, a fixed-wing UAV relay communication node was used. Specifically, the communication link between the relay node and the ground users was described using free-space pathloss model. The authors concentrated on the physical communication layer, link efficiency, message error rate, and the ground device handoff mechanism for switching between relay nodes.

Moreover, the topic of relay selection for UAV-assisted vehicular ad hoc networks (VANETs) was investigated in [13]. They investigate multi-UAV collaboration, the network communication node motion model, and the quality of service for air-to-surface connections for UAV relaying in VANETs.

In [14], the authors take advantage of two sleep-scheduling policies for massive machine-type communication devices, namely, the multiple vacation policy and the start-up threshold policy, which are defined in the context by three different multiple access protocols: time-division multiple access, frequency-division multiple access, and non-orthogonal multiple access. Furthermore, under the constraints of energy harvesting power, status update rate, and stability conditions, they develop closed-form formulas for the massive machine-type communication devices system's peak age of information (AoI), which are formulated as the optimization objective. By fixing the status update rate, an exact linear search-based approach is proposed for finding the optimal solution. A low-complexity concave-convex technique is also proposed as a design alternative for finding a near-optimal solution by transforming the original problem into a form represented by the difference of two convex problems. The authors in [15] study an AoI-energy-aware data collection system for UAV-assisted Internet of Things (IoT) networks using age of information as a performance metric to assess the temporal correlation among data packets consecutively sampled by the Internet of Things devices. By optimizing the UAV flight speed, hovering sites, and bandwidth allocation for data collection, they aim to reduce the weighted sum of predicted average AoI, UAV propulsion energy, and transmission energy at IoT devices. By adding a deep neural network for feature extraction, they develop a twin-delayed deep deterministic policy gradient-based UAV trajectory planning algorithm to deal with the multidimensional action space. In [16], the authors study an energy-efficient computation offloading technique for UAV-mobile-edge computing (MEC) systems with a focus on physical-layer security. For secure UAV-MEC systems, they design a set of energy-efficiency challenges, which are subsequently transformed into convex problems. Finally, the optimal solutions for both active and passive eavesdroppers are found.

Typically, in the exploration and search for minerals, the site to be analyzed in mining operations is first examined by the work team using geophysical equipment. This information is forwarded to the ground control station (GCs) for analysis, processing, and creating maps of the Earth's layers. Surveys are conducted in remote places where no telecommunication networks are available. As a result, the data acquired is kept and processed later at the GCs. Our research suggests a practical 3D placement of a dynamic UAV to operate as a relay node between the work team devices and the distant GCs over millimeter-wave frequencies in remote areas.

Because the surrounding environment in mining is typically harsh terrain, wireless communications network planning and enhancement is a challenging task. It differs from what communications engineers are used to when constructing wireless communications networks. In [17], they addressed the planning and optimization of broadband wireless networks in open-pit mines.

On the other hand, due to the constant change in topology and fleet in an open-pit mining environment, the study in [18] emphasizes the requirement for persistent wireless communication planning. Also, they provide an example of an LTE network that was planned and established in an open-pit mining site in 2007 to meet the needs of users and devices on the site, but in 2014 this network was no longer in service with only 34% of users; furthermore, the mine became more significant, and more areas needed to be connected by wireless communications.

Since working in an open-pit mine requires a collaborative system that includes mining people, sensors, and communications infrastructure. Rangan et al. discussed the possibility of a wireless emergency communications framework based on UAVs in deep open mines [19]. They found that, in open-pit mines, a UAV-based system has a viable communication method during an emergency and to bridge the coverage gap where there is no communication infrastructure. The rigorous performance evaluation of their proposed communications Skyhelp framework was implemented as a proof of concept.

1.1. Paper Contributions. The paper contributions are outlined as follows:

1 Two path losses models are utilized: The Air-to-Ground (ATG) pathloss model is utilized for the backhaul link. While, for the uplink, the Ground-to-Air pathloss model is used. These pathloss models are appropriate for 5G Aerial Millimeter Wave Networks.

2 The problem of determining the most efficient location and trajectory of a single UAV is addressed in order to optimize the total data rates of wireless devices in the scenario of uplink transmissions.

3 The RPGM mobility model is proposed and used to represent the users' movement inside the targeted

mining area and the PSO algorithm to find the efficient placements and trajectory for a UAV that maximizes the data rates of the wireless devices on uplink transmissions scenario.

The rest of this paper is structured as follows. In Section 2, the system model is presented. This section also includes the pathloss models for uplink and backhaul links. Section 3 presents the problem of determining an efficient UAV 3-D location and trajectory. Next, in Section 4, the Reference point group mobility model (RPGM) is presented. Then, Section 5 discusses the proposed UAV Placement and Trajectory Algorithm. After that, the simulation results are presented in Section 6. Finally, the conclusions are shown in Section 7.

2. System Model

Let the location of the aerial relay node is denoted by (x, y, z) and M wireless devices are assumed to be far away from the GCs. Due to the lack of line-of-sight linkages and substantial route losses caused by operating at high frequencies, these wireless devices are unable to communicate with the remote GCs. The drone, which works as an aerial relay node to convey information from the wireless devices to the GCs, must service the wireless devices, as illustrated in Figure 1. We assume an uplink situation in which the data is sent to the UAV using a frequency-division multiple access (FDMA) method with a signal-to-noise ratio (SNR) larger than or equal to SNR_{th} threshold.

This section considers a rectangular geographical region as a targeted mining area, $\mathbb{G} \subset \mathbb{R}^2$, this region is divided into n sub-regions $\mathscr{D} \in (n1, n2, \ldots, n_k)$, where $\mathscr{D}$ denoted as $(x_{\text{minimum}}, y_{\text{minimum}})$ and $(x_{\text{maximum}}, y_{\text{maximum}})$ as presented in Figure 2. More specifically, the users are distributed non-uniformly inside each sub-regions using beta random distribution and moving from sub-regions n to $n + 1$.

In this model, a single UAV serves and tracks mobile users during their movement inside the targeted region to accomplish the survey mission for mining. The UAV 3-D placement is represented by $(x_{uav}, y_{uav}, z_{uav})$ where (x_{uav}, y_{uav}) is the 2-D UAV placement and z_{uav} is the height of the UAV.

The mobile UAV can change its location to serve the ground users in the uplink scenario. We employ two mm wave pathloss models operating in 28 GHz in this scenario. The first model is the uplink model between users and UAV; the ground to air path model [20], and the second is between UAV and GCs [3]. Moreover, the RPGM mobility model represents the ground users' movement inside the targeted region.

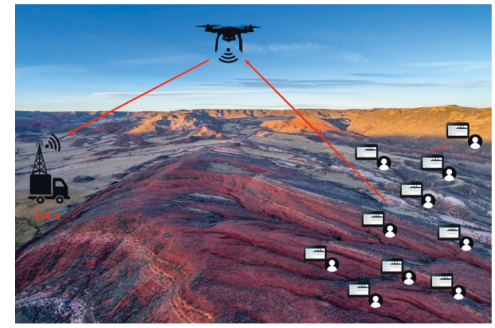

Figure 1: UAV acting as a relay node.

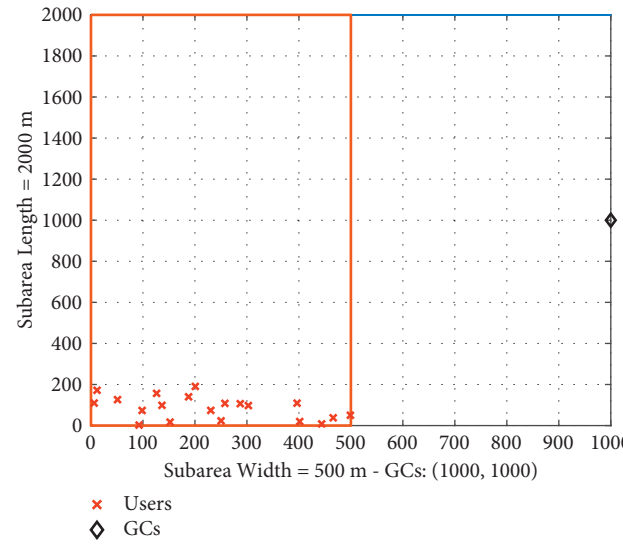

Figure 2: System settings of a coverage sub-area.

2.1. Path Loss Models. Millimeter waves technology can support bandwidth up to 2 GHz since it operates in an extremely high frequency (EHF) band, ranging from 28 GB to 100 GB, allowing multiple gigabit data rates transmission. Millimeter-wave technology is unsuitable for non-line of sight (NLOS) communication link scenarios for a relatively large distance due to the high signal attenuation, not only from buildings or barriers but also from being blocked by the human body [21]. But it is possible to use the millimeter-wave technique in cases where there are (NLOS) communication links at relatively small distances or in the LOS communication link for several kilometers.

In this research, we assume that a group of geologists are in the process of geological surveying and imaging the Earth's layers to detect minerals underground. There is a ground control station at a distance from them to process the data captured by exploration and prospecting devices. Since we use millimeter waves and do not have reliable LOS communication links with the ground control station, we use a UAV as a relay node between the wireless devices and the ground station. This study considers the uplink scenario between the ground users' devices and the UAV relay node.

2.2. Ground to Air Channel Model. We assume the survey team is working in semi-rugged terrain and providing data directly to the UAV relay node over millimeter waves in the case of uplink. To describe the channel between the ground users and the UAV relay node, we use the rural area route loss model. The mean pathloss between the i th user and UAV is given by [20, 22, 23].

$$L_{a,i} = P_L(r_i, z_u)L_{L,i} + [1 - P_L(r_i, z_u)]L_{N,i}, \quad (1)$$

where $L_{L,i}$ and $L_{N,i}$ are the pathlosses for LOS and NLOS links and they are given by

$$\begin{aligned} L_{L,i} &= A_L + 10B_L \log_{10}(d_i), \\ L_{N,i} &= A_N + 10B_N \log_{10}(d_i), \end{aligned} \quad (2)$$

where A_L, B_L, A_N, and B_N are the parameters of the line of sight (LOS) and non-line of sight (NLOS) pathloss models, and $d_i = \sqrt{(x_i - x_u)^2 + (y_i - y_u)^2 + (z_i - z_u)^2}$ is the 3D distance between the user and the UAV. Moreover, $P_L(r_i, z_u)$ represents the probability of human body blockage for the i th user and can be modeled as [23].

$$P_L(r_i, z_u) = \exp\left(-\lambda g_B \frac{r_i(h_B - h_R)}{(z_u - z_i)}\right), \quad (3)$$

where r_i is 2D distance between the i th user and the UAV, z_u is the height of the UAV, λ is the density of human blockers, g_B is the diameter of human blockers, h_B is the height of the human blocker, and z_i is the height of the user.

2.3. Air to Ground. Since we assumed the exploration and surveying operations take place in a remote area, we use the free space pathloss model to characterize communication channel between the UAV and the GCs. In free space pathloss model, L_{FS} the signal strength has a proportional relationship with the carrier frequency and the distance between the transmitter and the receiver, whereas the frequency or the distance increases, the pathloss will increase, as follows [3].

$$L_{\text{UAV-GC}}(d_{3\,D}) = 20\log_{10}(d_{3\,D}) + 20\log_{10}(f) + 92.45, \quad (4)$$

where $d_{3\,D} = \sqrt{(X_U - X_{GC})^2 + (Y_U - Y_{GC})^2 + (Z_U - Z_{GC})^2}$ is the 3D distance between the projection of the UAV and the GCs in Km, and f is the carrier frequency of the transmitted signal in GHz.

3. Problem Formulation

The problem of data rate maximization between ground users and the GCs via the UAV relay node is discussed in this work. As a result, we have two communication channels: one between ground users and the UAV and another between the UAV and the GCs. The data rate between a ground user i and the UAV can be calculated from Shannon's theorem as follows [24]:

$$C_{i-\text{UAV}} = B_{i-\text{UAV}} \log_2(1 + \text{SNR}_{i-\text{UAV}}), \quad (5)$$

where $B_{i-\text{UAV}}$ is the bandwidth assigned for ground user i, and $\text{SNR}_{i-\text{UAV}}$ is the signal-to-noise ratio of the received signal of ground user i at UAV relay node. However, the data rate between the UAV relay node and the GCs is given by

$$C_{\text{UAV}-GCs} = B_{\text{UAV}-GCs} \log_2(1 + \text{SNR}_{\text{UAV}-GCs}), \quad (6)$$

where $B_{\text{UAV}-GCs}$ is the bandwidth assigned for the communication channel between the UAV relay node and the GCs, and $\text{SNR}_{\text{UAV}-GCs}$ is the SNR of the UAV relay node transmitted signal at the GCs receiver.

This work aims to find an efficient placement and trajectory of a single UAV where the objective is to maximize the total data rate for ground nodes. The problem is formulated as follows:

$$x_u^t, y_u^t, z_u^t \sum_{i=1}^{|U|} \sum_{|T|} B_{i-\text{UAV}} \log_2\left(1 + \text{SNR}_{i-\text{UAV}}^t\right), \quad (7a)$$

$$\sum_{i=1}^{|U|} B_{i-\text{UAV}} \log_2\left(1 + \text{SNR}_{i-\text{UAV}}^t\right) \le B_{\text{UAV}-GCs} \log_2\left(1 + \text{SNR}_{\text{UAV}-GCs}^t\right), \forall t \in T, \quad (7b)$$

$$\text{SNR}_{i-\text{UAV}}^t \ge \text{SNR}_{th}, \forall i \in U, \forall t \in T, \quad (7c)$$

$$p_i^t \le p^{\max}, \forall i \in U, \forall t \in T, \quad (7d)$$

$$p_i^t \ge 0, \forall i \in U, \forall t \in T, \quad (7e)$$

$$x_{\min} \le X_u^t \le x_{\max}, \quad (7f)$$

$$y_{\min} \le Y_u^t \le y_{\max}, \quad (7g)$$

$$z_{\min} \le Z_u^t \le z_{\max}. \quad (7h)$$

Constraint (7b) is used to guarantee that the data rate for the connection between the drone and the ground wireless devices is less than or equal to the data rate of the connection between the GCs and the drone. The constraint (7c) is to

ensure that the devices' SNR is greater than or equal to the threshold. Moreover, constraint (7d) is used to ensure that the power consumption for each ground device is less than the maximum power for this device. The constraint (7e) is to ensure that the power consumption for each device is greater than or equal to zero. The constraints from (7f)–(7h) present the maximum and minimum X_u^t, Y_u^t, and Z_u^t values.

4. Mobility Model

Mobility models describe mobile nodes and users' movement patterns and mobility behavior. Moreover, it describes the location, velocity, and acceleration changes for users over time. Mobility models are split into two classes; individual movement models like a Random-Walk, or Brownian motion, Probabilistic Random Walk [25], Random Waypoint [26], Weighted Waypoint [27], and Random Directions [28]. The second category is group movement models such as Reference Point Group Model (RPGM) [29], Column Mobility Model, Nomadic Mobility Model, and Pursue mobility model [25]. RPGM illustrates the users' mobility inside the targeted mining area in this paper.

In RPGM model [29], the users' cluster has a centroid point, namely, logical reference point (RP). Moreover, all cluster members track the RP movement. Group RP's motion represents its behavior, with additional movement parameters such as the user's velocity, locations, direction, and acceleration. Hence, the group's trajectory is defined according to the RP movement. The group members are distributed uniformly near the reference point center within the targeted mining region.

For every time slot, the users' are moved inside the targeted sub-region and move from one sub-region to another by tacking the RP. The sub-region members are distributed randomly near the RP.

The RPGM model describes the mobility of group members for numerous approaches, such as in battleground communications and during catastrophe scenarios in search and rescue missions. In these systems, group members progress towards a common objective and create all users' cooperative movement.

The RPGM consists of RP (group centroid) and all group members inside the sub-region. The main components of this model will be represented as:

1 Reference point (RP): The RP guides the group member's movement, representing the group's motion pattern. Vector $\overrightarrow{V_{g(t)}}$ denotes the RP mobility of the group member's at time t and velocity v. The vector's path $\overrightarrow{V_{g(t)}}$ will be selected based on a predefined path or in a random manner. In this study, a predefined path to represent the member's trajectory is considered.

2 Group nodes: The RP movement will impact the mobility of the cluster members. The movement of each member is associated with the RP movement, which lets the cluster members heed the model movement. The allocation of group members is randomly distributed around the RP.

Group members represent the nodes located inside the sub-region of the team members.

The motion vector $\overrightarrow{Vel_{i(t)}}$ for member i at time t described as the following equation [30]:

$$\overrightarrow{Vel_{i(t)}} = \overrightarrow{Vel_{g(t)}} + G_{MV_i}(t), \tag{8}$$

where $G_{MV_i}(t)$ is the group motion vector of member i, and $\overrightarrow{Vel_{g(t)}}$ is the motion vector of the reference point.

5. UAV Placement and Trajectory Algorithm

In this section, the PSO algorithm [31, 32] is utilized to find the efficient UAV placement and trajectory such that the total data rate for all wireless devices in the uplink connection between all users and UAV is less than or equal to the total data rate for the backhaul connection between UAV and GCs. Specifically, the PSO algorithm is utilized to locate an efficient solution for the formulated problem in Section 3. Moreover, the proposed algorithm pseudo-code is presented in this section.

5.1. Particle Swarm Optimization Algorithm (PSO). Eberhart, Russell, and Kennedy proposed in [33] the PSO algorithm in 1995. PSO is a heuristic algorithm works based on the paradigm of a swarm and animal social behavior such as schools of fish and swarm of birds. In this algorithm, the swarm consists of n particles, and the particles communicate with each other for finding an efficient output to the formulated problem. During every iteration, the location and velocity of all particles are updated to better positions. The update process occurred according to the particles cost and the cost of their neighbors.

PSO is initialized with a set of n possible solutions (particles/members). Then, PSO updates the best local location and velocity for all particles/members according to velocity and position equations (9) and (10). In addition, PSO updates the global best location.

$$V_j(t+1) = V_j(t) + (k1 * r\text{and}) * \left(P_j^{\text{Best\_Loc}}(t) - P_j(t)\right) + (k2 * r\text{and}) * \left(P^{G\_Best}(t) - P_j(t)\right). \tag{9}$$

Here, $V_j(t+1)$ is the speed at $t+1$, $k1$ is the acceleration coefficients for best local solution. While, $k2$ is the acceleration coefficients global best solution. $r$and is a function used to generate a random number between 0 and 1, $P_j(t)$ is the location of the j_{th} particle/member, $P_j^{\text{Best\_Loc}}(t)$ is the best location of the j_{th} particle/member at time t, and $P^{G\_\text{Best}}(t)$ is the global best location of the problem.

The following equation presents the positions update for particle/member:

$$P_j(t+1) = P_j(t) + V_j(t+1). \tag{10}$$

The PSO algorithm is considered one of the most popular meta-heuristic algorithms. It can be used for finding or choosing a near-optimal solution to the optimization problem. PSO employs a global search method to locate the

Efficient UAV 3-D Placement
Input:
$(h_{\min}, h_{\max})$: min. and max. UAV height. $(x_{\min}, x_{\max})$, $(y_{\min}, y_{\max})$: MIN. and MAX. dimensionalities of the 2-D region.
Initialization: $z1$ = total_pathloss from users to UAV; $z2$ = total_pathloss from UAV to GCs;
For $(h = h_{\min} : h_{\max}, x = x_{\min} : x_{\max}, y = y_{\min} : y_{\max})$
for All users (U): *a*) Apply PSO to find 3-D UAV placement that minimizes z 1; *b*) Find z2;
end
If z1 $\leq$ z2, **then** $x_{\min} = x_{\min} + 1$;
Go to Step 3
else
Efficient 3-D UAV placement = (x, y, h)
end
(x, y, h) is the efficient 3-D UAV placement at minimum pathloss between users and UAV that satisfying the constraint in (7a).

Algorithm 1: Proposed algorithm for efficient UAV 3-D placement.

global optimal point instead of being stuck in a local minimum solution. Thus, the employment of the global search approach in PSO can overcome the problem of the local search methods that converges optimal local solutions. Moreover, it can converge to the efficient solution faster than other meta-heuristic algorithms [11].

5.2. Meta-Heuristic Algorithms Complexity. In this section, we present the computation complexity of two meta-heuristic algorithms, the PSO and the genetic algorithm GA. For PSO, the complexity depends on the following steps $a- Initialization of the population. b- Fitness function evaluation which requires t iterations. c- Performs N_{it} iterations for step b. d- Performs p_{it} iterations to update velocity and position for each particle. The worst-case complexity of these steps can be expressed as $\mathcal{O}(tp_{it}N_{it})$. For constant N_{it} the algorithm complexity is $\mathcal{O}(tp_{it})$.

On the other hand, the performance of the PSO-based approach is compared and evaluated against the GA algorithm. The computation complexity of the GA algorithm is discussed in detail in [30]. In GA, the fitness function of each particle of n population will be evaluated, then, the tournament selection to select m individuals that have the best fitness score, to become parents of the new generation of m individuals using the crossover and mutation process, will be evaluated. Specifically, in the tournament selection, it takes $\mathcal{O}(\log(m))$ operations, after building the initial tournament in $\mathcal{O}(m)$. Thus, considering the worst-case scenario, the computational complexity of the GA algorithm can be denoted as $\mathcal{O}(n.m\log(m))$.

The simulation results section presents the results for both PSO and GA algorithms, and we show that the PSO requires less computational complexity and less execution time.

5.3. Efficient UAV Placement Approach. This section discusses the proposed approach to find the efficient 3D UAV placement and trajectory such that the total group members throughput is maximized and satisfies the backhaul link throughput. Algorithm 1 presents the proposed approach. In this algorithm, we apply the PSO to solve the optimization problem and find the 3-D UAV placement that minimizes the total path losses between ground users and the UAV; then, we compare this pathloss with the backhaul pathloss between UAV and GCs. Here, we aim to guarantee that the total throughput between all users and UAV does not exceed the backhaul link throughput, specifically, to satisfy constraint 8a in the problem formulation. If the total pathloss between users and UAV is less than the backhaul link pathloss, then we move UAV 1 meter towards the GCs as in Step 5 in the proposed algorithm. These steps will be repeated until this constraint is satisfied.

6. Simulation Results and Discussion

In this section, the results of the proposed approach are presented. PSO is employed to find a UAV trajectory considering the mobility of the mining team, where their movement follows the RPGM models. In this paper, we aim to maximize the throughput of the mining team's members, satisfying the constraints in the problem formulation (7a)–(7h). The simulation parameters used in this work are presented in Table 1.

In this work, the dimension of the targeted mining region, $\mathbb{D}$ is 500 m × 2000 m. Moreover, the team members are uniformly distributed inside the sub-region and moving in a group based on RPGM model. In this scenario, the total number of team members is 20.

The total required time to finish the mining mission in each targeted area $\mathbb{G}$ is defined as T. Then, the targeted area $\mathbb{G}$ is split into n sub-areas, with dimensions of 500 m × 2000 m, where the 200 m is the sub-area length $\in\in\mathbb{D}$. The average movement speed of the team members is 0.41 m/s [30].

Figure 3 illustrates the movement of the mining team members from one sub-area to another at a speed of 0.41 m/s. Here, the worst-case distribution scenario for the mining team members inside sub-region k_n is considered. In this scenario, the users are distributed inside the whole k_n. Then, we find an efficient UAV placement, where the total path-losses between team members and the UAV are minimized, and guarantees that the total throughput between users and UAV does not exceed the backhaul link

Table 1: Simulation and system parameters.

Simulation and System Parameters					
Targeted mining area, $\mathbb{G}$	$(x_{\max}, y_{\max})$	(500 m, 2000 m)	Frequency	f	28 GHz
Min UAV height	$h_{\min}$	100 m	$(\alpha, \beta, \zeta \sim \mathcal{N}(0, \sigma^2))$	NLOS	(113.63, 1.16, 2.58)
Number of teams members	U	20	$(\alpha, \beta, \zeta \sim \mathcal{N}(0, \sigma^2))$	LOS	(84.64, 1.55, 0.12)
GCs location	(x_{GCs}, y_{GCs})	(1000, 1000)	PSO max # of iterations	N_{it}	100
Mining mission period	T	≃80 min	PSO population size	N_{pop}	50
Users velocity	V_i	≃0.41 m/sec	Height of GCs	hGCs	6 m
# Of sub-regions inside each $\mathbb{G}$	k	10	Noise power	Np	−100 dBm

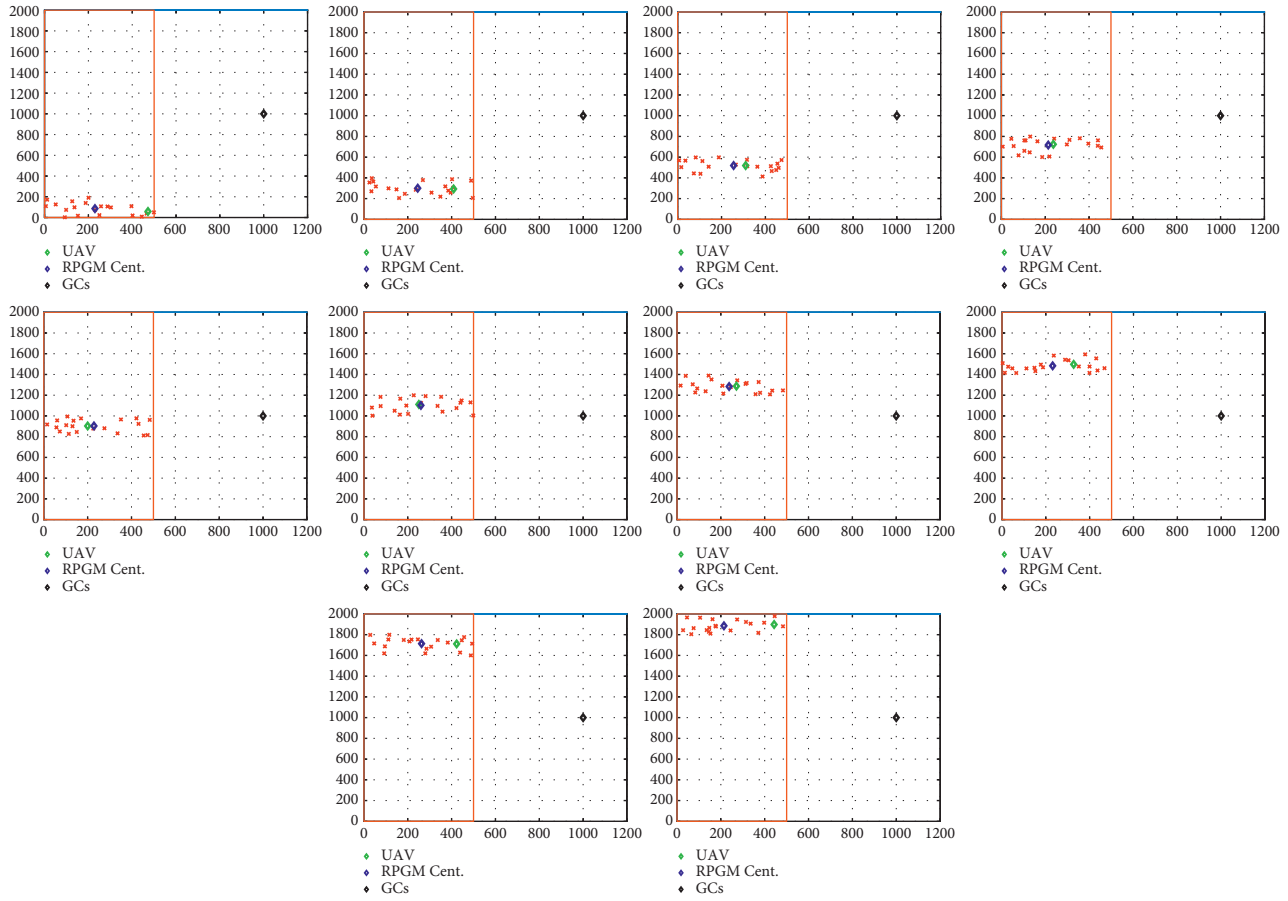

Figure 3: Users movement and trajectory based on RPGM inside the sub-area from T1 to T10. The dimensionalities of the axes are meters.

throughput. Specifically, this figure shows the users distribution, reference point for RPGM model, GCs, and the efficient 3-D UAV placement for each sub-region from T1 to T10.

As we can see in Figures 3–1, the sub-region dimensions $(0, 0)$ to $(500, 200)$, the mining team members starts forward movement from the beginning of the trajectory between $(0, 500)$ with velocity 0.41 m/s. The reference point for this sub-region is $(230, 86)$ as shown in Figures 3–1. The mining team members are distributed uniformly around this point. The time required to survey this sub-region is 8.1 minutes. Moreover, an efficient 3D UAV placement using PSO is $(472, 58.38, 100)$. This figure also presents the UAV 3-D placement and the reference point for the RPGM model for all time steps from T1 to T10.

Table 2 depicts the dimension of the sub-regions, the reference point of the RPGM model, the efficient 3-D UAV placement using two different heuristic algorithms PSO and GA. This table also presents the average pathloss for the uplink between team members and the aerial UAV; and the pathloss between UAV and the GCs for all time steps.

Moreover, from this table, it can be clearly seen that the PSO and GA algorithms converge to the same efficient placement. As a result, to compare these two meta-heuristic algorithms, we consider the execution time and the computational complexity for the worst-case scenario. On the other hand, the required time to find the efficient placement using GA is 1.9644 sec. Moreover, the PSO requires, on average, 1.6417 sec. Therefore, the PSO algorithm outperforms the GA in terms of execution time. The PSO reduces

Table 2: Simulation results for mining mission inside a subarea.

Time Step (T_n)	Alg.	Sub-region (m)	Efficient UAV 3-D Placement	Reference RPGM Model placement	Average pathloss Usr-UAV	Pathloss UAV-GCs
T1	PSO GA	0–200	(472, 58.379, 100) (470.22, 56.01, 102.74)	(230.81, 86.72, 0)	122.1563 122.1650	122.094
T2	PSO GA	200–400	(409, 293.248, 100) (409.3761, 293.6445, 100)	(245.38, 300.45, 0)	120.7329 120.7400	120.7300
T3	PSO GA	400–600	(310, 518.708, 100) (312.42, 520.07, 100)	(255.06, 519.13, 0)	120.0709 120.0714	119.9504
T4	PSO GA	600–800	(237, 723.795, 100) (239.10, 702.38, 100)	(213.89, 716.78,0)	119.8564 119.700	119.641
T5	PSO GA	800–1000	(200, 903.039, 100) (203.88, 908.61, 100.06)	(228.72, 903.46, 0)	119.6643 119.6856	119.5821
T6	PSO GA	1000–1200	(250, 1.1112e + 03, 100) (251.42 1.1112e + 03 100)	(260, 1101.8, 0)	119.6257 119.6258	119.0550
T7	PSO GA	1200–1400	(271, 1.2872e + 03, 100) (272.6354, 1.2923e + 03, 101.3710)	(237.8, 1283.5, 0)	119.3638 119.4084	119.3418
T8	PSO GA	1400–1600	(327, 1.4976e + 0,3 100) (328.40 1.4974e + 03 100)	(231.2, 1483.5, 0)	120.0784 120.0877	119.9063
T9	PSO GA	1600–1800	423, 1.7112e + 03, 100) (428.29 1.7084e + 03 100.54)	(262.9, 1713.5, 0)	120.7655] 120.8518	120.6787
T10	PSO GA	1800–2000	(443, 1.8982e + 03, 100) (454.91 1.8977e + 03 101.68)	(214.1, 1885.6, 0)	122.0125 122.2650	121.9112

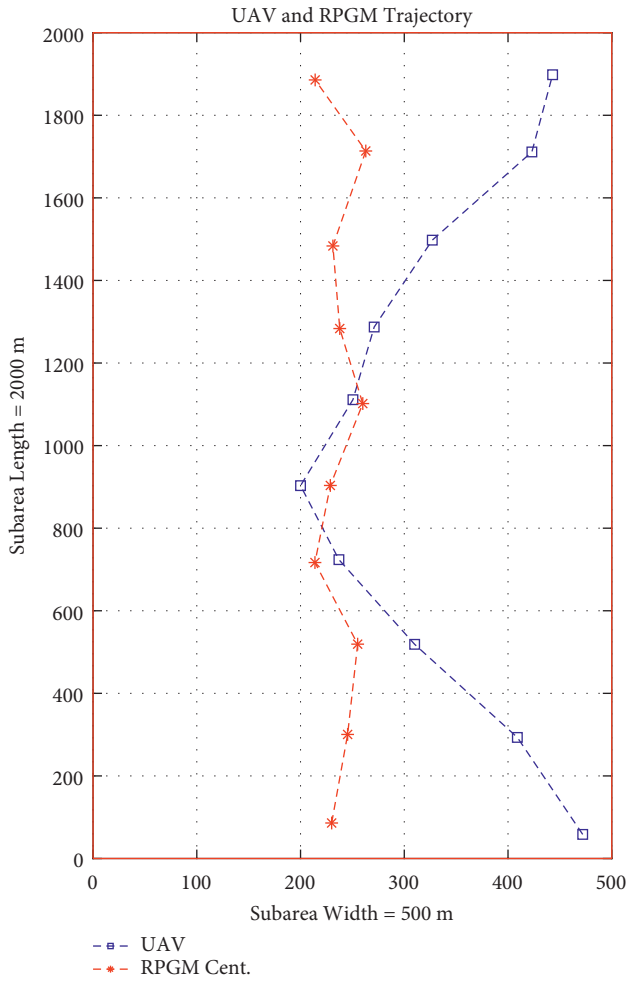

Figure 4: Efficient UAV and RPGM trajectories from T1 to T10.

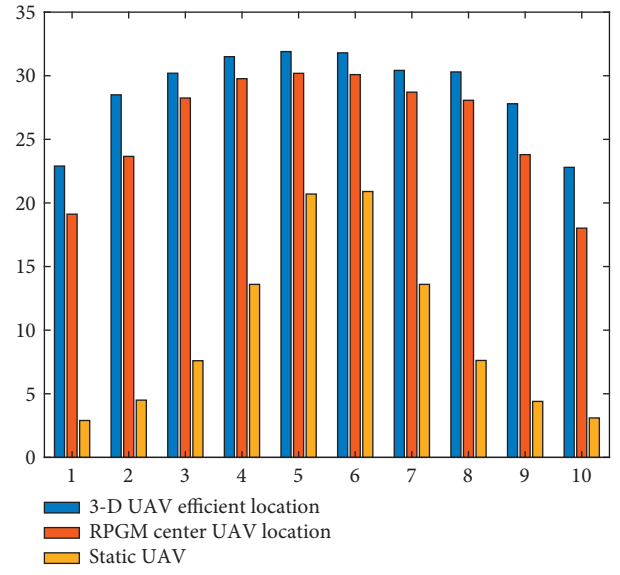

Figure 5: Users average sum rate over different time slots for 3 UAV placement approaches efficient, RPGM center and static.

the execution time by 16% compared to GA. In this paper, the minimum height of the aerial drone is 100 m for safety and collision avoidance. References [34, 35].

On the other hand, Figure 4 presents an efficient trajectory for the UAV during mining surveying operations from T_1 to T_10 using the proposed algorithm. Moreover, this figure shows the trajectory of the reference point for the RPGM model during team members' movement for all time slots.

Figure 5 shows the average sum rate of ground users for three different UAV placement scenarios, namely, dynamic, RPGM center, and static. Specifically, in the dynamic UAV

Table 3: Average sum rate for dynamic and static UAV locations.

Time step	Sub-region	Dynamic UAV sum rate	RPGM UAV sum rate	Static UAV sum rate
(T_n)	(m)	(bits/sec/Hz)	(bits/sec/Hz)	(bits/sec/Hz)
T1	(0–200)	22.9	19.12	2.9
T2	(200–400)	28.5	23.66	4.5
T3	(400–600)	30.2	28.25	7.6
T4	(600–800)	31.5	29.77	13.6
T5	(800–1000)	31.9	30.19	20.7
T6	(1000–1200)	31.8	30.09	20.9
T7	(1200–1400)	33.2	28.71	13.6
T8	(1400–1600)	30.3	28.07	7.6
T9	(1600–1800)	27.8	23.80	4.4
T10	(1800–2000)	22.8	18.02	3.1

placement scenario, the PSO algorithm is used to find the efficient trajectory of the UAV satisfying the constraints from (7b) to (7h). Then, in the static UAV placement, we consider the center of the coverage region $(500, 1000)$ as a location of the UAV. Moreover, for the third scenario, we use the center of the RPGM as a UAV placement from T1 to T10. In the second and third scenarios, the UAV height is set to 100 m. These two scenarios are employed as a benchmarking for comparison with the dynamic approach. As shown in Figure 5, the sum rate of team members in the dynamic UAV scenario outperforms both RPGM centers and static UAV scenarios for all time slots. Moreover, Table 3 presents the values of the average sum data rate for optimized dynamic UAV, RPGM centers, and static UAV locations [36].

7. Conclusion

UAVs in wireless communication networks have a great value on the mining industry. In this paper, a single UAV was used in the mining mission; specifically, UAV acted as a relay node between the exploration team and the GCs using millimeter-wave technologies. Two pathloss models were used to present the communication channel; the first is the ground to air pathloss to describe the uplink communication channel between the team members and the UAV that acts as a relay node. The second model is the free space pathloss, which is used to represent the downlink communication channel between the UAV and the GCs. The optimization problem was formulated with an objective function to find the 3-D location and trajectory of the UAV such that it maximizes the data rate of team members. Since the formulated problem is non-convex, we have used the PSO to find the UAV relay node's efficient 3D location and trajectory.

Data Availability

Data are available from the corresponding author upon request.

Conflicts of Interest

The authors declare that they have no conflicts of interest.

Acknowledgments

This work was supported by the Deputyship for Research and Innovation, Ministry of Education in Saudi Arabia, project no. 6864 2020 IF.

References

[1] H. Shakhatreh, A. H. Sawalmeh, A. Al-Fuqaha et al., "Unmanned aerial vehicles (uavs): a survey on civil applications and key research challenges," *IEEE Access*, vol. 7, no. 48, pp. 48572–48634, 2019.

[2] Y. Zeng, Q. Wu, and R. Zhang, "Accessing from the sky: a tutorial on uav communications for 5g and beyond," *Proceedings of the IEEE*, vol. 107, no. 12, pp. 2327–2375, 2019.

[3] L. Zhang, H. Zhao, S. Hou et al., "A survey on 5g millimeter wave communications for uav-assisted wireless networks," *IEEE Access*, vol. 7, no. 117, pp. 460–117 504, 2019.

[4] H. Ullah, N. G. Nair, A. Moore, C. Nugent, P. Muschamp, and M. Cuevas, "5g communication: an overview of vehicle-to-everything, drones, and healthcare use-cases," *IEEE Access*, vol. 7, no. 37, pp. 37251–37268, 2019.

[5] S. Yin, Z. Qu, and L. Li, "Uplink resource allocation in cellular networks with energy-constrained uav relay," in *Proceedings of the 2018 IEEE 87th Vehicular Technology Conference (VTC Spring)*, pp. 1–5, IEEE, Porto, Portugal, June 2018.

[6] U. Demir, C. Toker, and Ö. Ekici, "Energy-efficient deployment of uav in v2x network considering latency and backhaul issues," in *Proceedings of the 2020 IEEE International Black Sea Conference on Communications and Networking (BlackSeaCom)*, pp. 1–6, IEEE, Odessa, Ukraine, May 2020.

[7] S. Kumar, S. Suman, and S. De, "Backhaul and delay-aware placement of uav-enabled base station," in *Proceedings of the IEEE INFOCOM 2018-IEEE Conference on Computer Communications Workshops (INFOCOM WKSHPS)*, pp. 634–639, IEEE, Honolulu, HI, USA, May 2018.

[8] Y. Chen, W. Feng, and G. Zheng, "Optimum placement of uav as relays," *IEEE Communications Letters*, vol. 22, no. 2, pp. 248–251, 2017.

[9] H. Shakhatreh, A. Alenezi, A. Sawalmeh, M. Almutiry, and W. Malkawi, "Efficient placement of an aerial relay drone for throughput maximization," *Wireless Communications and Mobile Computing*, vol. 2021, Article ID 5589605, 11 pages, 2021.

[10] K. F. Hayajneh, K. Bani-Hani, H. Shakhatreh, M. Anan, and A. Sawalmeh, "3d deployment of unmanned aerial vehicle-base station assisting ground-base station," *Wireless*

Communications and Mobile Computing, vol. 2021, Article ID 2937224, 11 pages, 2021.

[11] S. Abdel-Razeq, H. Shakhatreh, A. Alenezi, A. Sawalmeh, M. Anan, and M. Almutiry, "Pso-based uav deployment and dynamic power allocation for uav-enabled uplink noma network," *Wireless Communications and Mobile Computing*, vol. 2021, Article ID 2722887, 17 pages, 2021.

[12] H. Shakhatreh, K. Hayajneh, K. Bani-Hani, A. Sawalmeh, and M. Anan, "Cell on wheels-unmanned aerial vehicle system for providing wireless coverage in emergency situations," *Complexity*, vol. 2021, Article ID 8669824, 9 pages, 2021.

[13] Y. He, D. Zhai, D. Wang, X. Tang, and R. Zhang, "A relay selection protocol for uav-assisted vanets," *Applied Sciences*, vol. 10, no. 23, p. 8762, 2020.

[14] Z. Fang, J. Wang, Y. Ren, Z. Han, H. V. Poor, and L. Hanzo, "Age of information in energy harvesting aided massive multiple access networks," *IEEE Journal on Selected Areas in Communications*, vol. 40, 2022.

[15] M. Sun, X. Xu, X. Qin, and P. Zhang, "Aoi-energy-aware uav-assisted data collection for iot networks: a deep reinforcement learning method," *IEEE Internet of Things Journal*, vol. 8, no. 24, pp. 17275–17289, 2021.

[16] T. Bai, J. Wang, Y. Ren, and L. Hanzo, "Energy-efficient computation offloading for secure uav-edge-computing systems," *IEEE Transactions on Vehicular Technology*, vol. 68, no. 6, pp. 6074–6087, 2019.

[17] L. G. U. Garcia, E. P. L. Almeida, V. S. B. Barbosa et al., "Mission-critical mobile broadband communications in open-pit mines," *IEEE Communications Magazine*, vol. 54, no. 4, pp. 62–69, 2016.

[18] V. S. Barbosa, L. G. Garcia, G. Caldwell et al., "The challenge of wireless connectivity to support intelligent mines," in *Proceedings of the 24th World Mining Congress 2016. IBRAM*, pp. 105–116, Brasília, Brazil, October 2016.

[19] A. Ranjan, B. Panigrahi, H. B. Sahu, and P. Misra, "Skyhelp: uav assisted emergency communication in deep open pit mines," in *Proceedings of the 1st International Workshop on Internet of People, Assistive Robots and Things*, pp. 31–36, Munich, Germany, June 2018.

[20] H. Shakhatreh, W. Malkawi, A. Sawalmeh, M. Almutiry, and A. Alenezi, "Modeling ground-to-air path loss for millimeter wave uav networks," 2021, https://arxiv.org/abs/2101.12024.

[21] X. Wang, L. Kong, F. Kong et al., "Millimeter wave communication: a comprehensive survey," *IEEE Communications Surveys & Tutorials*, vol. 20, no. 3, pp. 1616–1653, 2018.

[22] M. R. Akdeniz, Y. Liu, M. K. Samimi et al., "Millimeter wave channel modeling and cellular capacity evaluation," *IEEE Journal on Selected Areas in Communications*, vol. 32, no. 6, pp. 1164–1179, 2014.

[23] M. Gapeyenko, I. Bor-Yaliniz, S. Andreev, H. Yanikomeroglu, and Y. Koucheryavy, "Effects of blockage in deploying mmwave drone base stations for 5g networks and beyond," in *Proceedings of the 2018 IEEE international conference on communications workshops (icc workshops)*, pp. 1–6, IEEE, Kansas, MO, USA, May 2018.

[24] D. Tse and P. Viswanath, *Fundamentals of Wireless Communication*, Cambridge University Press, Cambridge, England, UK, 2005.

[25] T. Camp, J. Boleng, and V. Davies, "A survey of mobility models for ad hoc network research," *Wireless Communications and Mobile Computing*, vol. 2, no. 5, pp. 483–502, 2002.

[26] J. Broch, D. A. Maltz, D. B. Johnson, Y.-C. Hu, and J. Jetcheva, "A performance comparison of multi-hop wireless ad hoc network routing protocols," in *Proceedings of the 4th annual ACM/IEEE international conference on Mobile computing and networking*, pp. 85–97, ACM, Dallas , TX, USA, October 1998.

[27] W.-j. Hsu, K. Merchant, H.-w. Shu, C.-h. Hsu, and A. Helmy, "Weighted waypoint mobility model and its impact on ad hoc networks," *ACM SIGMOBILE - Mobile Computing and Communications Review*, vol. 9, no. 1, pp. 59–63, 2005.

[28] P. Nain, D. Towsley, B. Liu, and Z. Liu, "Properties of random direction models," in *Proceedings of the IEEE 24th Annual Joint Conference of the IEEE Computer and Communications Societies*, vol. 3, pp. 1897–1907, Miami, FL, USA, March 2005.

[29] K. H. Wang and B. Li, "Group mobility and partition prediction in wireless ad-hoc networks," in *Proceedings of the 2002 IEEE International Conference on Communications. Conference Proceedings. ICC 2002 (Cat. No.02CH37333)*, vol. 2, pp. 1017–1021, Philadelphia, Pennsylvania, April 2002.

[30] A. H. Sawalmeh, N. S. Othman, H. Shakhatreh, and A. Khreishah, "Wireless coverage for mobile users in dynamic environments using uav," *IEEE Access*, vol. 7, pp. 126 376–126 390, 2019.

[31] J. Kennedy and R. Eberhart, "Particle swarm optimization,"vol. 4, pp. 1942–1948, in *Proceedings of the ICNN'95-International Conference on Neural Networks*, vol. 4, pp. 1942–1948, IEEE, Perth, WA, Australia, November 1995.

[32] M. Clerc and J. Kennedy, "The particle swarm - explosion, stability, and convergence in a multidimensional complex space," *IEEE Transactions on Evolutionary Computation*, vol. 6, no. 1, pp. 58–73, 2002.

[33] R. Eberhart and J. Kennedy, "A new optimizer using particle swarm theory," in Micro Machine and Human Science," in *Proceedings of the 6th International Symposium on 1995 MHS'95*, pp. 39–43, IEEE, Lugano, Switzerland, October 1995.

[34] A. Sawalmeh and N. S. Othman, "An overview of collision avoidance approaches and network architecture of unmanned aerial vehicles (UAVs)," *International Journal of Engineering and Technology*, vol. 7, no. 4, p. 35, 2018.

[35] M. A. Jasim, H. Shakhatreh, N. Siasi, A. Sawalmeh, A. Aldalbahi, and A. Al-Fuqaha, "A survey on spectrum management for unmanned aerial vehicles (uavs)," *IEEE Access*, vol. 10, 2021.

[36] M. Anam, K. P. Rane, A. Alenezi, R. Mishra, S. Ramamurthy, and F. J. J. Joseph, "Content classification tasks with data preprocessing manifestations," *Webology*, vol. 19, no. 1, 2022.